Electronic Supplementary Material (ESI) for Journal of Materials Chemistry C.

Electronic Supporting Information (ESI)

for

A Healable Waterborne Polyurethane Synergistically Cross-Linked by Hydrogen Bonds and Covalent Bonds for Composite Conductor

Yan Yang, Zushan Ye, Xiaoxuan Liu*, Jiahui Su*

Guangdong Provincial Key Laboratory of Functional Soft Condensed Matter,

Department of Polymeric Materials and Engineering,

School of Materials and Energy, Guangdong University of Technology, Guangzhou, PR China.

*Corresponding authors. Email address: p-xxliu@gdut.edu.cn (X. Liu)

*Corresponding authors. Email address: sujiahuigdut@outlook.com (J. Su)

Experimental Procedures

Characterization

Average particles size and Zeta potential of latexes were measured by dynamic light scattering (DLS) using Brookhaven Zeta PALS particle size analyzer. The latexes were first diluted with deionized water about 1 vol.% before test. Thermogravimetric analysis (TGA) was conducted between 30 and 600 °C on a Mettler TGA/SDTA 851 instrument in N_2 atmosphere with a heating rate of 10 °C/min. Solid-state ^{1}H NMR spectrum was obtained through a Bruker AVANCE III 600 MHz Superconducting FT NMR SPECTROMETER (600 MHz, MAS probe: 1.0 mm, spinning frequency: 15 kHz) at room temperature. Tensile properties were performed by using a CMT4204 testing machine (MTS, American) at a crosshead speed of 50 mm/min at ambient temperature in accordance with the specification of the Chinese National Standard GB/T1040.3×2006. The dumbbell-shaped specimens were prepared with the neck dimensions of 4 mm, effective length of 25 mm and thickness of 0.3-0.4 mm. The specimens were analyzed at least three trails to obtain the average values. SEM was used to observe the micro-structure of the composite to demonstrate the interfacial adhesion by Hitachi S-4800 electron microscope. The test voltage was 15 kV.

The solid content of WPU-U_xH_y emulsion

The solid content of WPU-U_xH_y emulsion was determined according to Eq. (1):

$$X\,\% = \left[(W_0 - W_1)/W_0\right] \times 100 \quad (1)$$

Where W_0 is the weight of emulsion before curing and W_1 is the weight of emulsion after curing.

Emulsion stability properties of WPU-U_xH_y emulsion

Storage stability was evaluated for six months by observing the appearance and property of the latex.

Mechanical stability: the latex was poured into a tube and then centrifuged at 3000 r/min for 30 min in a TG1650-WS centrifuge (Lu Xiangyi Centrifuge Instrument Co. Ltd, China). The latex was place vertically for 48 h to observe the appearance and property of the latex.

Dynamic-mechanical properties of WPU-U_xH_y cured film

Dynamic thermomechanical analysis (DMA) was performed by a Metravib DMA50 apparatus. The storage modulus (E') and loss factor (tan δ) were measured from -30 °C to 140 °C using a heating rate of 3 °C/min at 1 Hz frequency with a tensile displacement of 10^{-5} m in a tensile configuration. The effective crosslinking density (v_c) could be calculated by the rubber elastic theory evolution equation (2), where v_c has the following relationship with the storage modulus E' of the rubber platform region:

$$v_c = {E'}/{3RT} \quad (2)$$

Where E' is the storage modulus at 298 K, v_c is crosslinking density, R is gas constant, and T is absolute temperature.

Self-healing properties of WPU-U_xH_y cured film

The self-healing behavior of WPU-U_xH_y cured film was performed as following methods.

For the surface scratch damage healing analysis, the scar was made with a razor blade on the surface of the cured films, and the films were then placed in the oven at different temperature for different time to heal the damage. The healing process was observed by an optical microscope (BKPOL, Chongqing, China).

For mechanical healing analysis, the dumbbell-shaped specimens were cut with a razor blade from the middle, the fresh cut surfaces were pressed compactly and left at different temperature for different time before tensile testing. The healed sample was conducted on stretching experiment again. The healed sample was conducted on tensile test again. Healing efficiency (*HE %*) was calculated according to the following equation:

$$HE\,\% = \frac{\delta_{repaired}}{\delta_{origin}} \times 100\% \quad (3)$$

Where $\sigma_{repaired}$ and σ_{origin} represent the tensile strength or elongation at break for healed and the pristine specimens, respectively.

The dynamic rheological properties were obtained by a HAAKE rotary rheometer (Thermo, Germany) with 20 mm stainless steel parallel plate under axial force of 0.1 N. Using the Oscillation model at 1 Hz, strain amplitude from 0.1 to 10% was determined to lie within the linear viscoelastic region (LVR) and the strain amplitude dynamic alternating scan test was performed on the cured film at different temperature following the programmed procedure: at 80 °C 0.1% (90 s) -50% (60 s) -0.1% (300 s) -50% (60 s) -0.1% (300 s) -50% (60 s) -0.1% (300 s) -50% (60 s) -0.1% (300 s) -50% (60 s) -0.1% (300 s); At 100 °C, the large deformation was altered into 100%.

Energy dissipation analysis of WPU-U_xH_y cured film

Incremental loading and unloading cycles were performed with the same experimental setup as tensile tests at 100 mm/min. During self-recovery testing, the loading-unloading cycles were performed as following methods: at the fatigue-accumulation test ten successive loading–unloading cycles were performed without any time delay at the fixed 100% strain and 100 mm/min, and then repeated with delays of 5, 15, 30 and 60 min respectively.

Electrical characteristics

Selecting 3~5 points as the average, the square resistance of the conductor was measured using a standard four-point probe method (Four Probe Technology Co., Ltd. China) at room temperature with 1 mA current.

Results and Discussion

Table. S1 Molar ratio of UPy to HEMA

Sample	WPU-U_6H_4	WPU-U_7H_3	WPU-U_8H_2	WPU-U_9H_1	WPU-U_0H_{10}
UPy (mol)	0.036	0.042	0.048	0.054	0
HEMA (mol)	0.024	0.018	0.012	0.006	0.06
UPy : HEMA	6 : 4	7 : 3	8 : 2	9 : 1	0 : 10

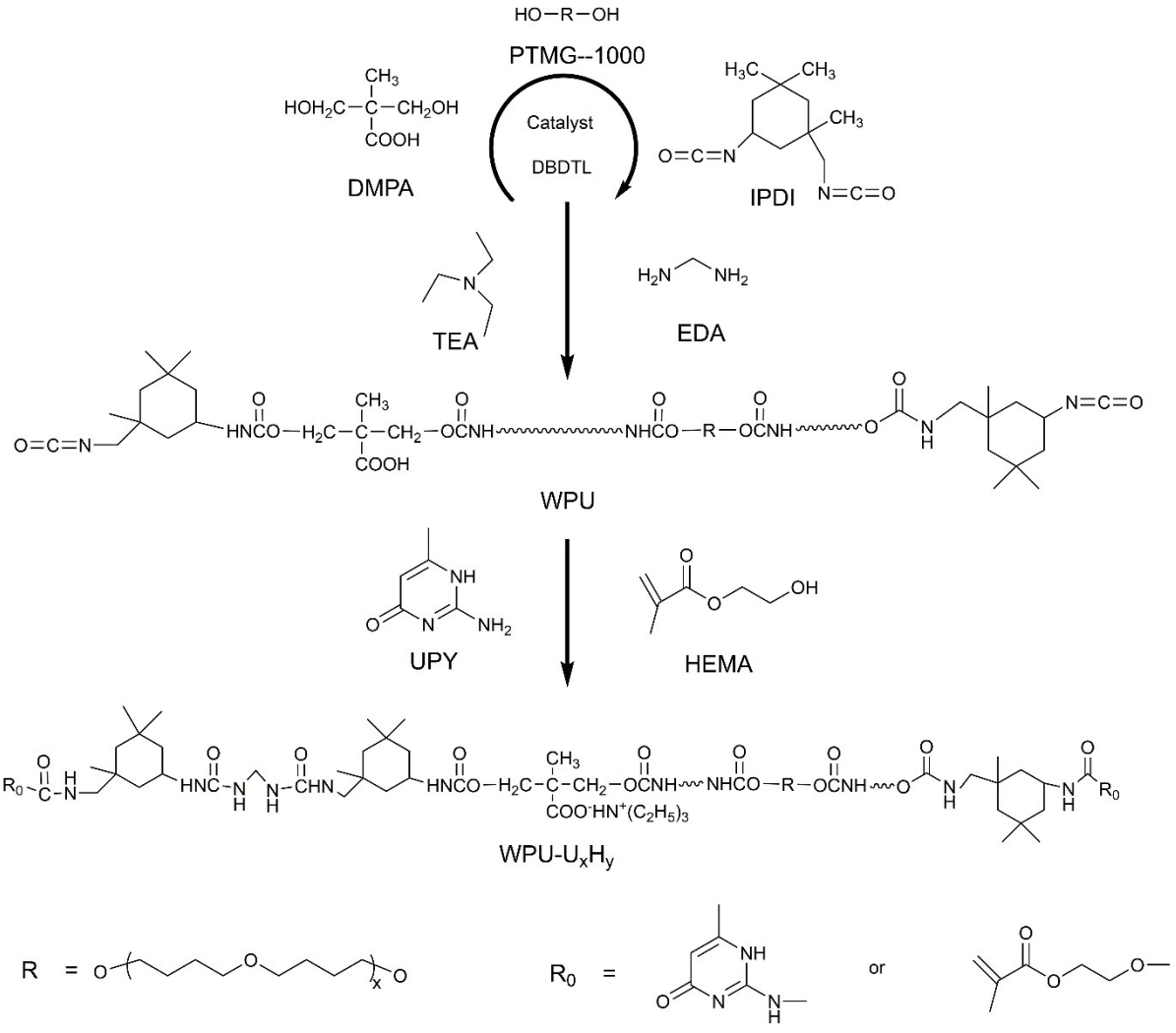

Scheme. S1 Synthesis route of WPU-U_xH_y emulsion

Table. S2 Effect of ratio of UPy to HEMA on the performance of WPU-U_xH_y emulsion

Sample	Solid content (%)	Average particles size (nm)	Polydispersity indexes	Zeta potential (mV)	Mechanical stability	Storage stability
WPU-U_9H_1	31.67	29.3	0.121	-49.79	Stable	Stable
WPU-U_8H_2	32.55	38.6	0.128	-56.18	Stable	Stable
WPU-U_7H_3	31.93	31.9	0.136	-58.12	Stable	Stable
WPU-U_6H_4	32.48	31.2	0.148	-66.96	Stable	Stable
WPU-U_0H_{10}	31.34	34.2	0.099	-75.49	Stable	Stable

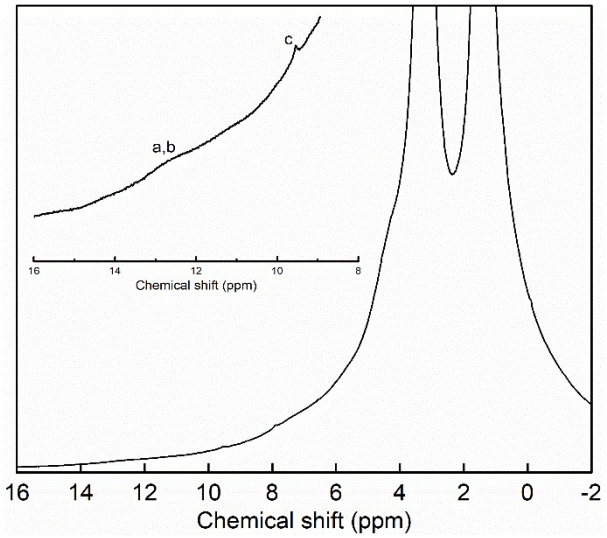

Fig. S1 Solid-state ^{1}H NMR spectrum of WPU-U_7H_3 cured film

Table. S3 Results of tensile texting of WPU-U_xH_y cured films

Sample	Tensile stress (MPa)	Elongation at break (%)	Yield strength (MPa)
WPU-U_9H_1	7.44±0.63	625.75±50.86	2.15±1.73
WPU-U_8H_2	9.88±0.76	606.21±32.91	3.32±1.14
WPU-U_7H_3	13.71±1.66	546.15±44.66	3.81±1.19
WPU-U_6H_4	22.92±2.01	495.67±21.79	6.27±1.34
WPU-U_0H_{10}	35.46±3.76	268.10±2.45	—

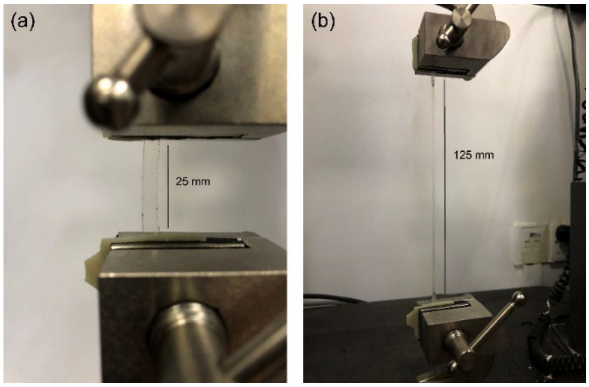

Fig. S2 The photographs of WPU-U_7H_3 cured film: (a) before stretching; (b) stretching to 500% of its initial length

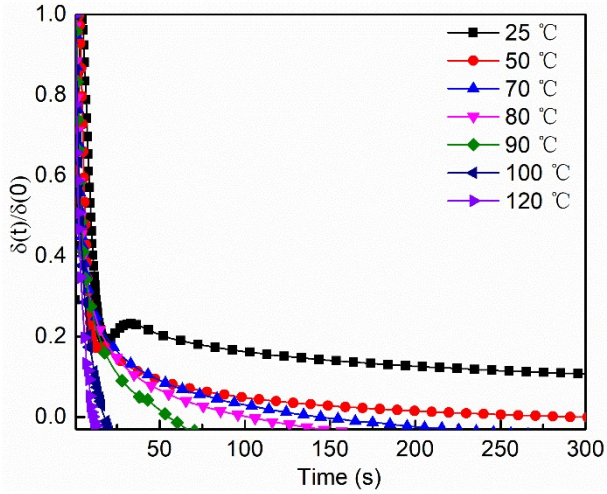

Fig. S3 Stress relaxation of WPU-U_7H_3 cured film

Table. S4 DMA results of the WPU-U_xH_y cured films

Sample	tan δ	$T_{max,\ tan\ \delta}$ (°C)[a]	Effectively damped temperature range (tan δ > 0.3) (°C)	The damping peak width ΔT (°C)	ν_{25} (10^{-4} mol·cm^{-3})[b]
WPU-U_9H_1	0.72	84.95	32 ~ 112	80	1.32
WPU-U_8H_2	0.70	86.46	33 ~ 140	107	2.08
WPU-U_7H_3	0.69	87.41	39 ~ 128	89	3.72
WPU-U_6H_4	0.67	92.88	54 ~ 117	64	4.64
WPU-U_0H_{10}	0.56	86.65	50 ~ 112	62	5.28

[a] the temperature corresponding to the highest peak value of tan δ; [b] Cross-linking density of the cured film at 25 ℃

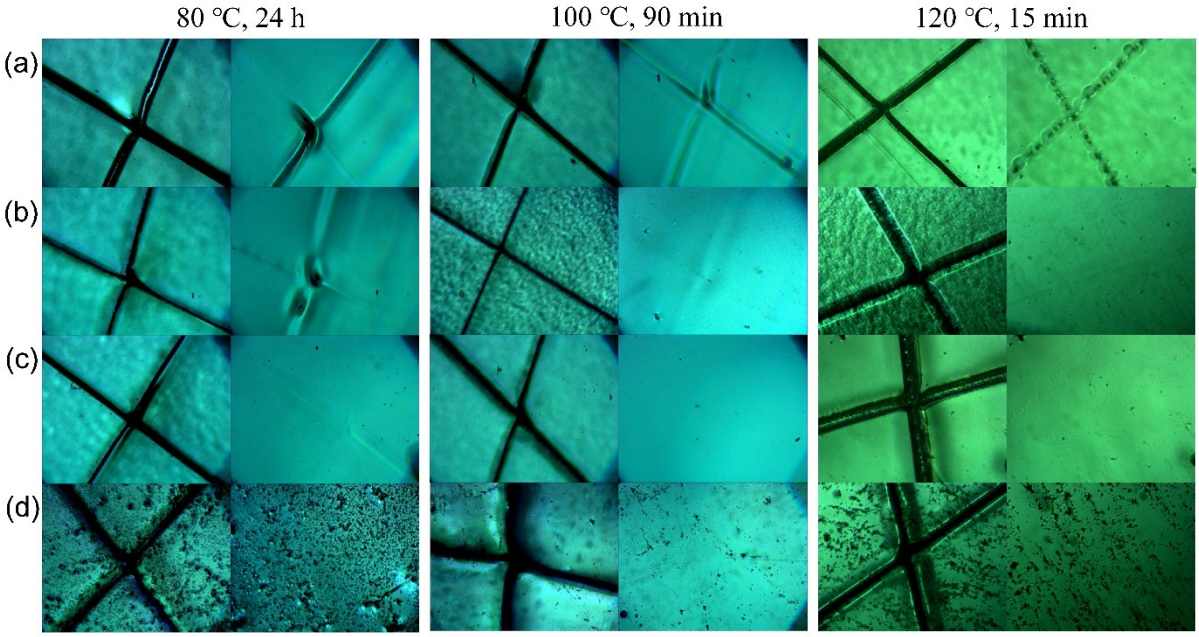

Fig. S4 Optical microscopy images of the scratched WPU-U_xH_y cured films before and after self-healing: (a) WPU-U_6H_4; (b) WPU-U_7H_3; (c) WPU-U_8H_2; (d) WPU-U_9H_1

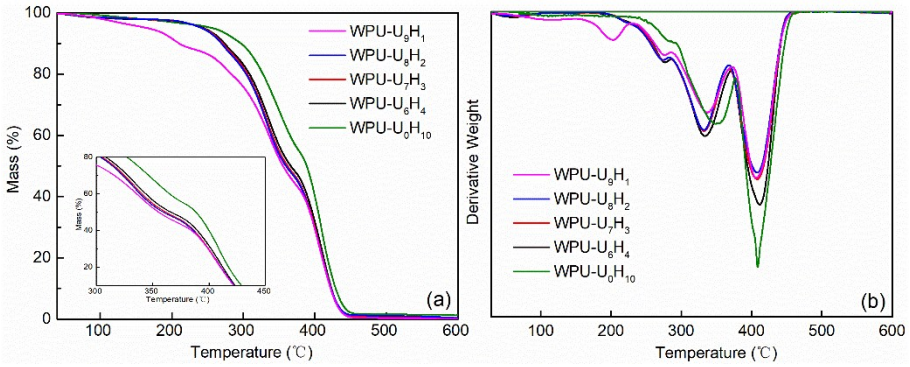

Fig. S5 Thermal properties of the WPU-U_xH_y cured films

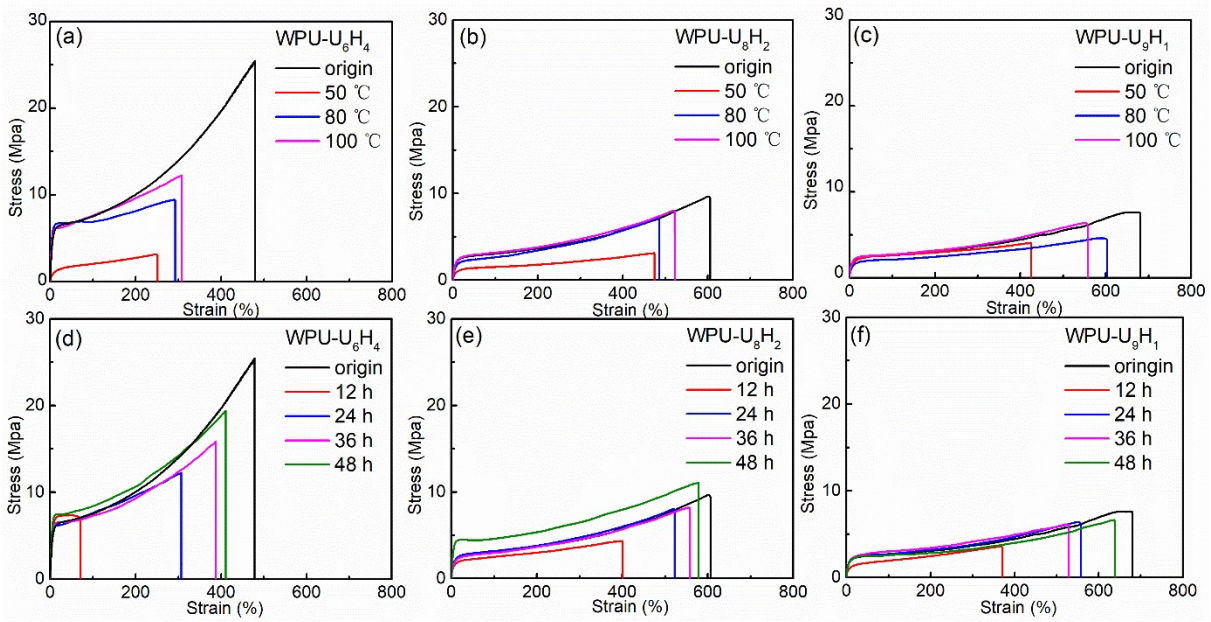

Fig. S6 Tensile curves of the self-healed WPU-U_xH_y cured films at different temperatures for 24 h: (a) WPU-U_6H_4; (b) WPU-U_8H_2; (c) WPU-U_9H_1;

Tensile curves of the self-healed WPU-U_xH_y cured films at 100 °C for different time: (d) WPU-U_6H_4; (e) WPU-U_8H_2; (f) WPU-U_9H_1

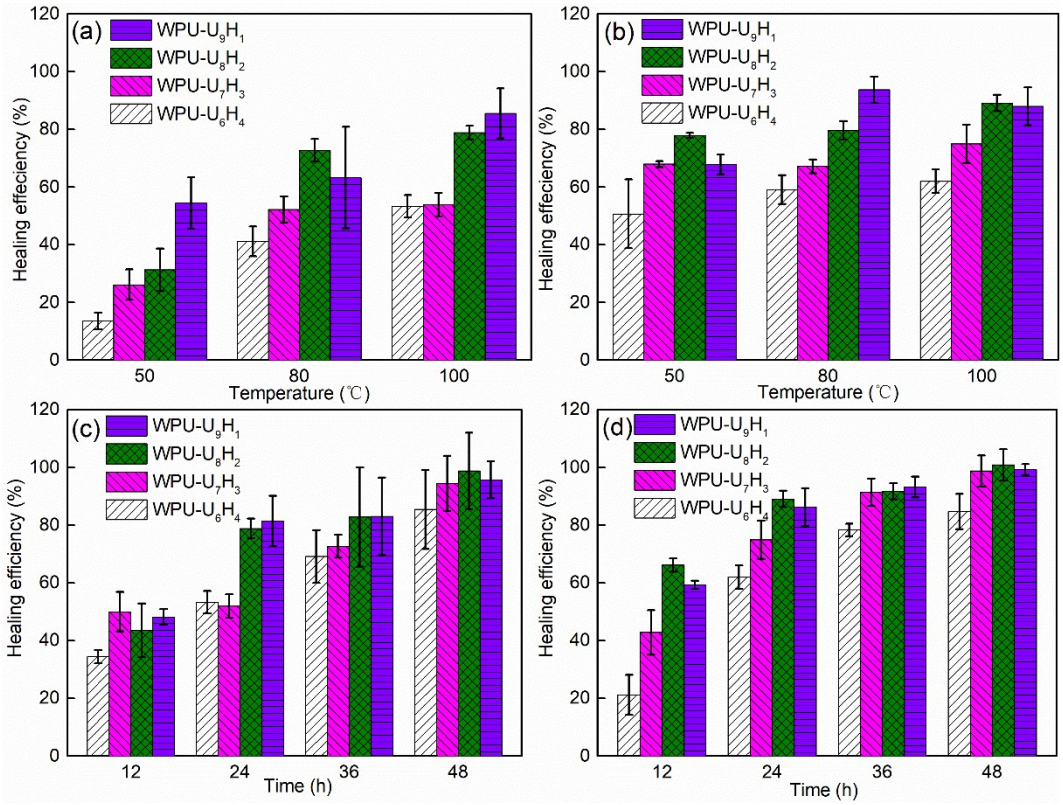

Fig. S7 The healing efficiency of tensile properties of the WPU-U_xH_y cured films: at different temperature for 24 h (a) tensile strength and (b) elongation at break; at 100 °C for different time (c) tensile strength and (d) elongation at break

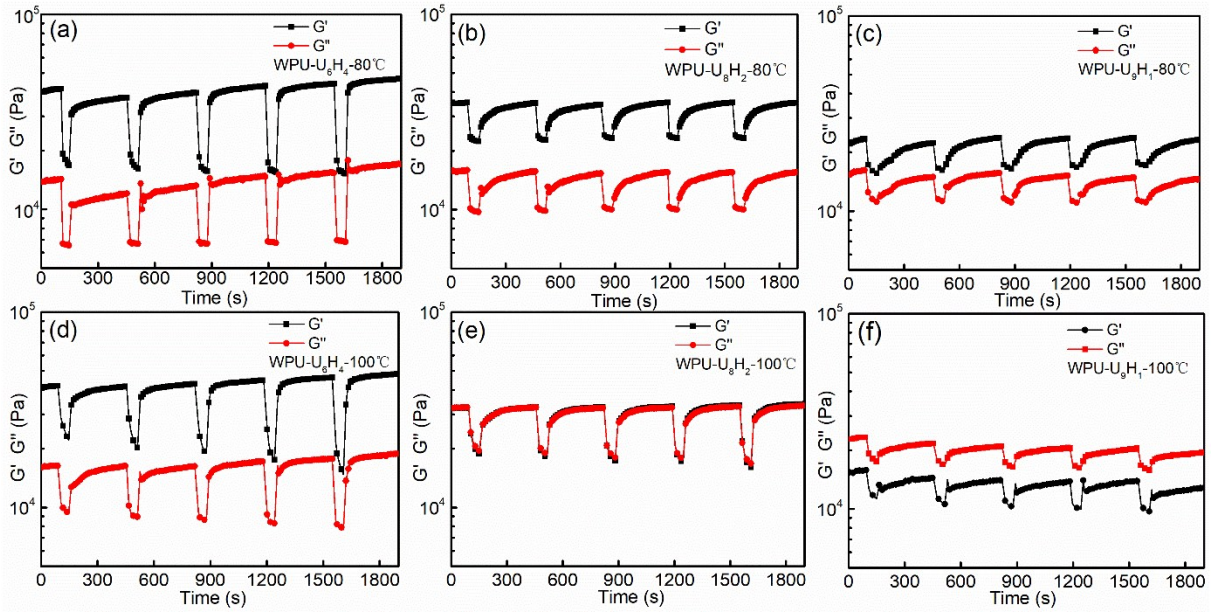

Fig. S8 (a)-(c) Dynamic strain amplitude cyclic test at 80 °C (γ = 1% or 50%); (d)-(f) Dynamic strain amplitude cyclic test at 100 °C (γ = 1% or 100%)

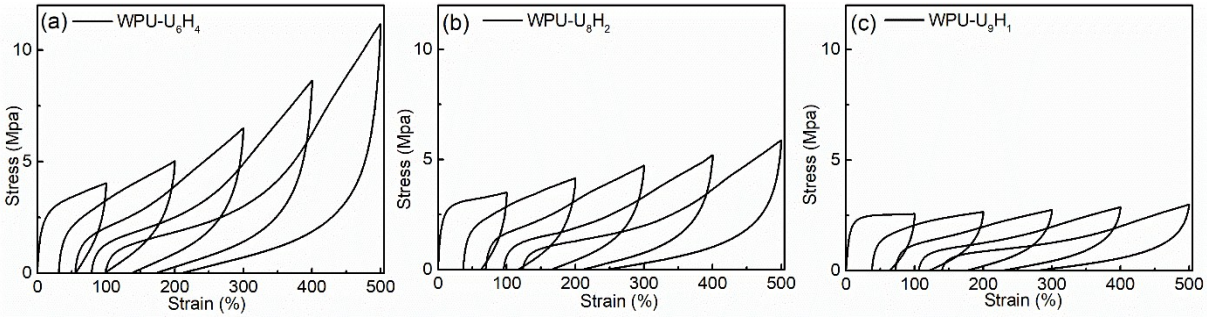

Fig. S9 Stress-strain curves for the step-cycle (strain: 100%-500%): (a) WPU-U_6H_4; (b) WPU-U_8H_2; (c) WPU-U_9H_1

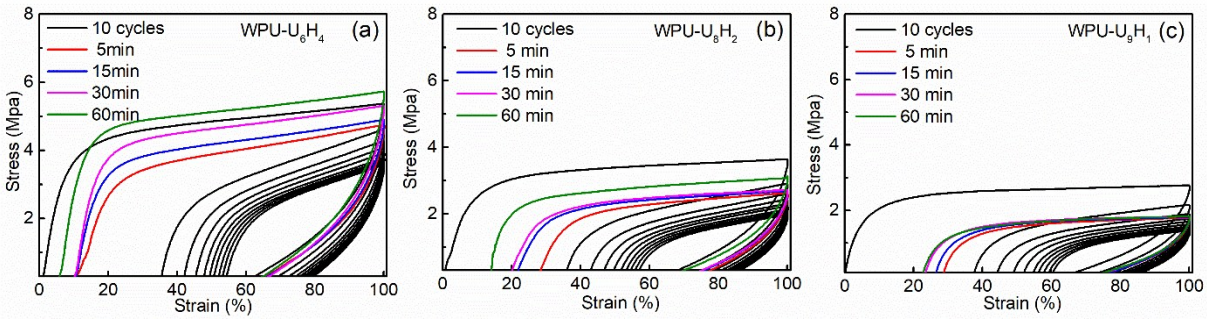

Fig. S10 Stress-strain curves fixed at 100% strain after different waiting time: (a) WPU-U_6H_4; (b) WPU-U_8H_2; (c) WPU-U_9H_1

Table. S5 The effect of ACET content on the conductivity of the WPU-U_7H_3 conductor

ACET (wt.%)[a]	Square resistance (Ω)
5	—
10	2670.63±72.58
15	256.00±1.63

[a] wt.% (mass fraction) is the percentage of the content of ACET to resin

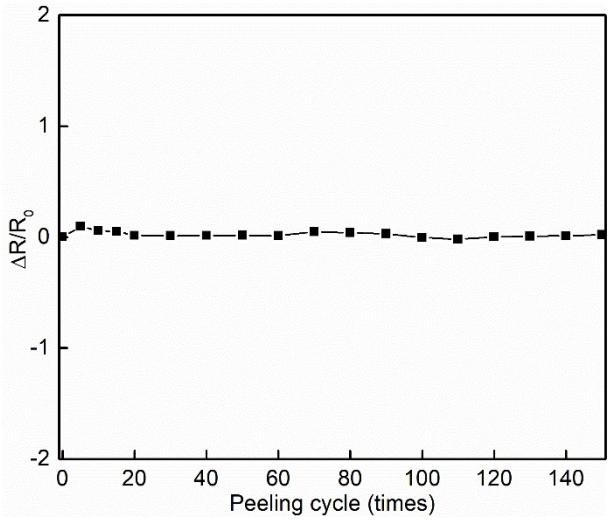

Fig. S11 The relative resistance changes of the WPU-U_7H_3@ACET composite conductor on the repeated adhesion and peeling test with 3M adhesive tape

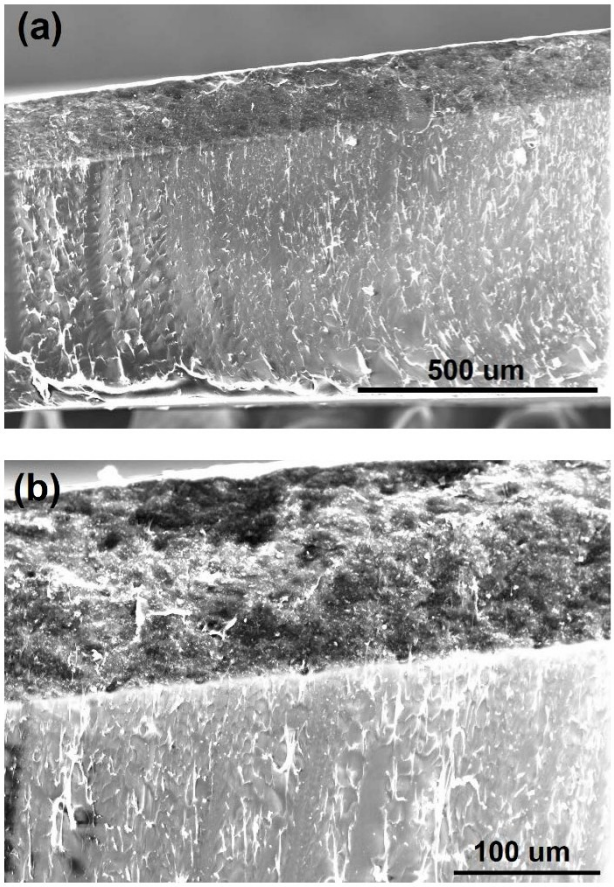

Fig. S12 SEM images of the micro-structure of the WPU-U_7H_3@ACET composite conductor to demonstrate the interfacial adhesion